J|A|C|S
ARTICLES
Published on Web 09/08/2005

Electrochemical and Chemical Formation of $[Mn_4^{IV}O_5(terpy)_4(H_2O)_2]^{6+}$, in Relation with the Photosystem II Oxygen-Evolving Center Model $[Mn_2^{III,IV}O_2(terpy)_2(H_2O)_2]^{3+}$

Carole Baffert,[†] Sophie Romain,[†] Aurélien Richardot,[†] Jean-Claude Leprêtre,[†] Bertrand Lefebvre,[‡] Alain Deronzier,*[,†] and Marie-Noëlle Collomb*[,†]

Contribution from the Laboratoire d'Electrochimie Organique et de Photochimie Rédox, Université Joseph Fourier-UMR CNRS 5630, Institut de Chimie Moléculaire de Grenoble, FR CNRS 2607, BP 53, 38041 Grenoble Cedex 9, France, and Centre de Recherches du Service de Santé des Armées "Emile Pardé", Laboratoire de Biospectrométrie, 24 Avenue des Maquis du Grésivaudan, BP 87, 38702 La Tronche, Cedex, France

Received April 21, 2005; E-mail: Marie-Noelle.Collomb@ujf-grenoble.fr; Alain.Deronzier@ujf-grenoble.fr

Abstract: To examine the real ability of the binuclear di-μ-oxo complex $[Mn_2^{III,IV}O_2(terpy)_2(H_2O)_2]^{3+}$ (**2**) to act as a catalyst for water oxidation, we have investigated in detail its redox properties and that of its mononuclear precursor complex $[Mn^{II}(terpy)_2]^{2+}$ (**1**) in aqueous solution. It appears that electrochemical oxidation of **1** allows the quantitative formation of **2** and, most importantly, that electrochemical oxidation of **2** quantitatively yields the stable tetranuclear Mn^{IV} complex, $[Mn_4^{IV}O_5(terpy)_4(H_2O)_2]^{6+}$ (**4**), having a linear mono-μ-oxo$\{Mn_2(\mu\text{-oxo})_2\}_2$ core. Therefore, these results show that the electrochemical oxidation of **2** in aqueous solution is only a one-electron process leading to **4** via the formation of a mono-μ-oxo bridge between two oxidized $[Mn_2^{IV,IV}O_2(terpy)_2(H_2O)_2]^{4+}$ species. **4** is also quantitatively formed by dissolution of the binuclear complex $[Mn_2^{IV,IV}O_2(terpy)_2(SO_4)_2]$ (**3**) in aqueous solutions. Evidence of this work is that **4** is stable in aqueous solutions, and even if it is a good synthetic analogue of the "dimers-of-dimers" model compound of the OEC in PSII, this complex is not able to oxidize water. As a consequence, since **4** results from an one-electron oxidation of **2**, **2** cannot act as an efficient homogeneous electrocatalyst for water oxidation. This work demonstrates that a simple oxidation of **2** cannot produce molecular oxygen without the help of an oxygen donor.

Introduction

The biological generation of dioxygen from water during photosynthesis (eq 1) occurring through photosystem II (PSII) is one of the most important and fundamental chemical processes in nature.[1,2]

$$2H_2O \rightarrow O_2 + 4H^+ + 4e^- \qquad (1)$$

In PS II, this four-electron oxidation is catalyzed by the oxygen-evolving center (OEC) containing a μ-oxo-bridged manganese tetramer associated with Ca^{2+} and Cl^- ions. In the proposed catalytic cycle of Kok et al.,[3] based on the works of Joliot et al.,[4] the Mn_4 cluster cycles through five distinct oxidation states (S_{states}: S_0 to S_4). The most oxidized one, S_4, is unstable and relaxes back to S_0 with the release of O_2. However, despite intensive spectroscopic studies on this enzyme which proposed Mn oxidation states in the range II−IV for the S_0 to S_3 states[2,5−8] and recent resolutions at 3.8, 3.7, and 3.5 Å of the X-ray structures of PSII,[9−11] the mechanism of water oxidation remains elusive as well as the exact structure of the Mn_4 cluster.

To mimic this natural active center, many high-valent multinuclear μ-oxo bridged manganese complexes have been synthesized.[2,12,13] However only few studies relative to their reactivity toward water oxidation have been published, and none of them described a nonambiguous example of an active catalyst. On the other hand, some related systems based on ruthenium complexes have been shown to be capable of oxidizing water to molecular oxygen.[14] Among these very few systems is the

[†] Université Joseph Fourier.
[‡] Laboratoire de Biospectrométrie.

(1) Photosynthetic water oxidation: Special Dedicated Issue; Nugent, J., Ed. *Biochim. Biophys. Acta* **2001**, *1503*, 1.
(2) Mukhopadhyay, S.; Mandal, S. K.; Bhaduri, S.; Armstrong, W. H. *Chem. Rev.* **2004**, *104*, 3981.
(3) Kok, B.; Forbush, B.; McGloin, M. *Photochem. Photobiol.* **1970**, *11*, 457.
(4) Joliot, P.; Barbieri, G.; Chabaud, R. *Photochem. Photobiol.* **1969**, *10*, 309.
(5) Yachandra, V. K. *Philos. Trans. R. Soc. London, Ser. B: Biol. Sci.* **2002**, *357*, 1347.
(6) Sauer, K.; Yachandra, V. K. *Proc. Natl. Acad. Sci. U.S.A.* **2002**, *99*, 8631.
(7) Yachandra, V. K.; Sauer, K.; Klein, M. P. *Chem. Rev.* **1996**, *96*, 2927.
(8) Britt, R. D.; Peloquin, J. M.; Campbell, K. A. *Annu. Rev. Biophys. Biomol. Struct.* **2000**, *29*, 463.
(9) Zouni, A.; Witt, H.-T.; Kern, J.; Fromme, P.; Krauβ, N.; Saenger, W.; Orth, P. *Nature (London)* **2001**, *409*, 739.
(10) Kamiya, N.; Shen, J.-R. *Proc. Natl. Acad. Sci. U.S.A.* **2003**, *100*, 98.
(11) Ferreira, K. N.; Iverson, T. M.; Maghlaoui, K.; Barber, J.; Iwata, S. *Science* **2004**, *303*, 1831.
(12) Yagi, M.; Kaneko, M. *Chem. Rev.* **2001**, *101*, 21.
(13) Ruettinger, W.; Dismukes, G. C. *Chem. Rev.* **1997**, *97*, 1.
(14) Deronzier, A.; Moutet, J.-C. In *Comprehensive Coordination Chemistry II*; Cleverty, J. A., Meyer, T. J., Eds.; Elsevier Pergamon: Oxford, 2004; Vol. 9, Chapter 10, p 471.

10.1021/ja052595+ CCC: $30.25

μ-oxo blue dimer *cis,cis*-$[(bpy)_2(H_2O)Ru^{III}ORu^{III}(OH_2)(bpy)_2]^{4+}$ (bpy = 2,2′-bipyridine) and its derivatives.[15] The mechanism of water oxidation is highly complex, since it involves the sequential four-electron oxidation in aqueous solutions of the aquo complex $(H_2O)Ru^{III}ORu^{III}(OH_2)$ to the oxo one $(O{=})Ru^{V}$-$ORu^{V}({=}O)$, followed by water oxidation. This oxidation can be achieved electrochemically or in the presence of Ce^{IV}. However, in the homogeneous phase, the turnover numbers are low because of anation induced by O_2 evolution. Recently, the first example of a dinuclear Ru complex, $[(terpy)_2(H_2O)Ru^{II}$-$(bpp)Ru^{II}(OH_2)(terpy)_2]^{4+}$ (terpy = 2,2′:6′,2″-terpyridine, Hbpp = 3,5-di(2-pyridyl)pyrazole)), capable of oxidizing water to O_2 that does not contain the Ru−O−Ru motif was reported.[16] The redox properties of this complex are radically different from those of the blue dimer due mainly to the absence of the Ru−O−Ru group. Indeed, the active species is the oxo complex $(O{=})Ru^{IV}Ru^{IV}({=}O)$, obtained by a four-electron stepwise oxidation of the initial $(H_2O)Ru^{II}Ru^{II}(OH_2)$ complex by an electrochemical way or with Ce^{IV}. The overall performance of this complex is remarkably superior to that of the blue dimer due to the *in,in* configuration of the oxo ligands and to a lower competitive anation side reaction.

Concerning the manganese chemistry, Brudvig, Crabtree, and co-workers,[17] reported that O_2 is evolved by the reaction of Mn^{II} and Mn^{III} mononuclear $[Mn(L)_2]^n$ complexes containing the planar tridentate ligands terpyridine ($n = +2$, complex (**1**)) or dipicolinate ($n = -1$) with potassium peroxymonosulfate (oxone, $KHSO_5$) in an acetate buffer solution at a pH lower than 4. This reaction produces a di-μ-oxo $Mn_2^{III,IV}$ dimer as a green intermediate. However, in the case of the dpa complex, the formation of MnO_4^- from the green species occurs concomitantly with O_2 evolution causing termination of the catalytic process. The terpy complex is far more robust with a largely higher turnover since, in contrast to the dpa system, there is no building up of MnO_4^-. Subsequently, the green intermediates corresponding to the $[Mn_2^{III,IV}O_2(terpy)_2(H_2O)_2]^{3+}$ complex (**2**) was synthesized and structurally characterized by their and our group.[18,19] Brudvig and co-workers[18] reported also that **2** can catalyze water oxidation when sodium hypochlorite (NaOCl) is used as a primary oxidant. This was the first report of a di-μ-oxo complex, a structural model for the manganese complex in the OEC, which could carry out catalytic O−O bond formation. However, the real source of oxygen atoms for O_2 evolution remains questionable. $KHSO_5$ and NaOCl are highly oxidizing oxygen-atom transfer reagents and O_2 could originate entirely from the oxidants rather than water. To clearly identify the source of oxygen atoms, ^{18}O isotope-labeling experiments of water with both oxidants ($Na^{16}OCl$ and $KHS^{16}O_5$) were carried out.[20] The ^{16}O atom of OCl^- exchanges rapidly with ^{18}O of water making $Na^{18}OCl$ unsuitable for $H_2{}^{18}O$ labeling experiments. In the case of oxone, this exchange is slow and the maximum of $^{36}O_2$ obtained is 12%, depending on the relative concentration of **2** and oxone. The rate-limiting step for O_2 evolution is proposed to be the formation of an $(H_2O)Mn^{IV}O_2$-$Mn^{V}{=}O$ intermediate that can exchange with water and then competitively react with either oxone or water/hydroxide to produce O_2. Nevertheless no evidence of the existence of such an intermediate was provided in their studies in order to confirm the proposed mechanism.

To exclude the possibility of the participation of the oxidizing agent in the oxygen atom source, experiments should be conducted using oxidizing agents that do not contain any oxygen atoms. Recently it has been reported that the reaction of **2** with a Ce^{IV} oxidant evolved no O_2 in homogeneous solution.[21] However surprisingly, these authors report that when **2** is adsorbed into Kaolin clay, the addition of a large excess of Ce^{IV} to the resulting aqueous suspension produces a significant amount of O_2.

To have a better understanding of the real capability of **2** to act as a catalyst for water oxidation, we have investigated in detail the electrochemical behavior of **1** and **2** in aqueous solution. Since the electrode exchanges only electrons, if some O_2 evolution occurs, the source of oxygen atoms will be undoubtedly water. We will see that the electrochemical oxidation of **1** allows the quantitative formation of **2** and, most importantly, that electrochemical oxidation of **2** allows the quantitative buildup of the stable tetranuclear Mn^{IV} complex, $[Mn_4^{IV}O_5(terpy)_4(H_2O)_2]^{6+}$ (**4**), having a linear mono-μ-oxo-$\{Mn_2(\mu\text{-oxo})_2\}_2$ core. This complex has been very recently chemically prepared using oxone as the chemical oxidant and crystallographically characterized as perchlorate salt.[22]

In parallel we have examined the behavior of the binuclear complex $[Mn_2^{IV,IV}O_2(terpy)_2(SO_4)_2]$ (**3**)[20] in aqueous media and demonstrated that this complex undergoes a quite rapid evolution into the tetranuclear Mn^{IV} complex **4**.

Finally, we explored the possibilities of inducing the oxidation of **2** photochemically.

Experimental Section

Materials. Bidistilled water was used for electrochemistry experiments. The ligand 2,2′:6′,2"-terpyridine (terpy, 99.9%, Acros), $[Ru^{II}$-$(bpy)_3](Cl)_2$, $[Co^{III}(NH_3)_5Cl](Cl)_2$, and $Na_2(S_2O_8)$ (Aldrich) were used as received. The electrolytes $NaNO_3$, K_2SO_4, Na_2SO_4 (Prolabo), KCF_3-SO_3, $NaCF_3SO_3$, $NaClO_4$ (Fluka), $NaCF_3CO_2$, $NaBF_4$ (Aldrich), and KPF_6 (Acros) were used without further purification.

Instrumentation. Electrochemical measurements were carried out using an EG&G PAR model 173 potentiostat equipped with a 179 digital coulometer and a model 175 programmer with output recorded on a Sefram TGM 164 X-Y recorder.

In aqueous medium, electrochemical experiments were performed in unbuffered solutions containing 0.1 M of $NaNO_3$, Et_4NNO_3, K_2-SO_4, Na_2SO_4, KCF_3SO_3, $NaCF_3SO_3$, $NaCF_3CO_2$, or $NaBF_4$ as supporting electrolytes. The pH values of the resulting solutions are comprised between 3 and 4. Electrochemical experiments were also performed in buffered terpy/terpyH$^+$ (the total concentration [terpy] + [terpyH$^+$] was 0.005 M) aqueous solutions containing 0.1 M of Na_2SO_4. The most clearly defined cyclic voltammograms were obtained with $NaCF_3SO_3$ or $NaBF_4$ as an additional supporting electrolyte. The Ag/AgCl/3 M KCl was used as the reference electrode. The potential referenced to that system can be converted to the SCE by adding 20 mV. Working electrodes for cyclic voltammetry and exhaustive electrolysis were, respectively, a vitreous carbon disk (3 or 5 mm in diameter) carefully polished with diamond paste and rinsed with ethanol before each

(15) Binstead, R. A.; Chronister, C. W.; Ni, J.; Hartshorn, C. M.; Meyer, T. J. *J. Am. Chem. Soc.* **2000**, *122*, 8464.
(16) Sens, C.; Romero, I.; Rodriguez, M.; Llobet, A.; Parella, T.; Benet-Buchholz, J. *J. Am. Chem. Soc.* **2004**, *126*, 7798.
(17) Limburg, J.; Brudvig, G. W.; Crabtree, R. H. *J. Am. Chem. Soc.* **1997**, *119*, 2761.
(18) Limburg, J.; Vrettos, J. S.; Liable-Sands, L. M.; Rheingold, A. L.; Crabtree, R. H.; Brudvig, G. W. *Science* **1999**, *283*, 1524.
(19) Collomb, M.-N.; Deronzier, A.; Richardot, A.; Pecaut, J. *New J. Chem.* **1999**, *23*, 351.
(20) Limburg, J.; Vrettos, J. S.; Chen, H.; de Paula, J. C.; Crabtree, R. H.; Brudvig, G. W. *J. Am. Chem. Soc.* **2001**, *123*, 423.
(21) Yagi, M.; Narita, K. *J. Am. Chem. Soc.* **2004**, *126*, 8084.

potential run and a carbon felt piece (10 × 10 × 4 mm^3; RCV 2000 from Le Carbone Lorraine). Previous attempts to examine the cyclic voltammogram with a platinum working electrode in this medium failed owing to the large background current from the competing oxidation of water.

X-band electron paramagnetic resonance (EPR, 9.4 GHz) spectra were recorded with a Brucker ESP 300 E spectrometer between 100 and 170 K, with the following parameters: microwave 1 mW, modulation amplitude 0.197 G, time constant 327.68 ms, scan rate 1342 s, scan width 8 G, modulation frequency 100 kHz. Low-temperature EPR spectra (from 4 to 77 K) were recorded on an X-band Bruker EMX spectrometer equipped with an Oxford Instruments ESR-900 continuous-flow helium cryostat and an ER-4116 OM Bruker cavity.

UV−visible spectra were obtained using a Cary 100 absorption spectrophotometer on 0.1 or 1 cm path length quartz cells. The electrospray ionization mass spectrometry (ESI-MS) experiments were performed on a triple quadrupole mass spectrometer Quattro II (micromass, Altrincham, UK). The ESI source was heated to 90 °C. The sampling cone voltage was set to 15 V. Complexes in solution (2.5 to 3 mM in H_2O) were injected using a syringe pump at a flow rate of 10 μL min^{-1}. The electrospray probe (capillary) voltage was optimized to 2.3 kV for positive electrospray. IR spectra were recorded on a Magna-IR TM 550 Nicolet spectrometer.

Irradiation. The irradiation experiments have been performed using a mercury lamp (Oriel 66901) (250 W) whose UV and IR radiation was cut off with filters. The aqueous solutions (pH 3) were constituted by a mixture of $[Ru^{II}(bpy)_3]^{2+}$ (1 mM), $[Mn_2^{III,IV}O_2(terpy)_2(H_2O)_2]^{3+}$ (1 mM), and $[Co^{III}(NH_3)_5Cl]^{2+}$ or $S_2O_8^{2-}$ (15 mM). With $S_2O_8^{2-}$, the aqueous solution was buffered with 0.1 M ClAcOH/$ClAcO^-$.

Synthesis. The complexes $[Mn_2^{III,IV}O_2(terpy)_2(H_2O)_2](NO_3)_3{\cdot}6H_2O$ (**2**·$(NO_3)_3$·$6H_2O$), $[Mn_2^{IV,IV}O_2(terpy)_2(SO_4)_2]{\cdot}6H_2O$ (**3**·$6H_2O$), and $[Mn_4^{IV}O_5(terpy)_4(H_2O)_2](ClO_4)_6{\cdot}3H_2O$ (**4**·$(ClO_4)_6$·$3H_2O$) were prepared according to the litterature.[18−20, 22]

$[Mn^{II}(terpy)_2](NO_3)_2$ (1). This complex was obtained according to a method similar to that described previously for the synthesis of $[Mn^{II}(terpy)_2](BF_4)_2$, except that $Mn(NO_3)_2{\cdot}4H_2O$ was used instead of $Mn(O_2CCH_3)_2{\cdot}4H_2O$. A solution of 0.065 g of $Mn(NO_3)_2{\cdot}4H_2O$ (0.25 mmol) in 2.5 mL of H_2O was added to 0.117 g of terpy (0.5 mmol) in 2.5 mL of acetone. The resulting yellow solution was stirred for 15 min and filtered to remove any impurities and then concentrated by rotary evaporation in a vacuum to obtain a yellow precipitate. The yellow solid was filtered off, washed with diethyl ether, and then dried in a vacuum. Yield: 0.174 g (70%).

IR in cm^{-1} (KBr): ν = 3444 (m); 3056 (w); 2921 (w); 1598 (s); 1577 (m); 1479 (m); 1454 (s); 1439 (s); 1384 (s); 1338 (vs); 1247 (m); 1190 (w); 1161 (m); 1091 (w); 1012 (s); 828 (w); 772 (vs); 650 (m); 638 (m); 517 (w); 490 (w); 425 (w); 401 (w).

Results and Discussion

I. Electrochemistry. The electrochemical oxidation of $[Mn_2^{III,IV}O_2(terpy)_2(H_2O)_2]^{3+}$ (**2**) (and also $[Mn^{II}(terpy)_2]^{2+}$ (**1**) via **2**; see further in the text) can a priori lead to two kinds of species. In the first case the formed species contains Mn with the +V oxidation state and a terminal oxo group instead of an aqua one, as suggested by Brudvig and co-workers.[17,18,20] The electrochemical behavior of **2** in this case should be somewhat reminiscent to that of the $[Ru_2^{III,III}O(bpy)_4(H_2O)_2]^{2+}$ complex.[15] The other possibility involves the formation of a high nuclearity oxo manganese complex building from aggregation of the electrogenerated $[Mn_2^{IV,IV}O_2(terpy)_2(H_2O)_2]^{4+}$ species in a close fashion to what was observed previously for the electrooxidation of the $[Mn_2^{III,IV}O_2(L)_4]^{3+}$ (L= bpy, phen (1,10-phenanthroline)) complexes[23−25] containing two bidentate nitrogen ligands L per manganese instead of a tridentate one. For these complexes, aggregation implies the decoordination of one ligand L per dimer and the interaction with water to produce the stable tetranuclear complexes $[Mn_4^{IV}O_6(L)_6]^{4+}$ (Scheme 1).

Scheme 1. Formation of $[Mn_4^{IV}O_6(L)_6]^{4+}$ by Electrochemical Oxidation of $[Mn_2^{III,IV}O_2(L)_4]^{3+}$ (L= bpy or phen) in Aqueous Buffered Solutions at pH 4.5 (L/LH^+ 0.05 M) (E = Electrochemical Step, C = Chemical Step)

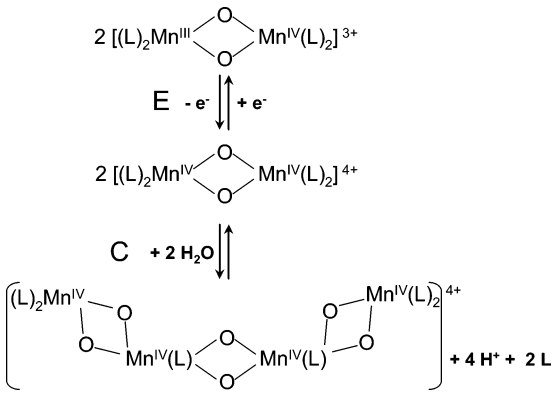

As previously reported,[19] **2** is soluble and stable for several hours in aqueous solutions in the presence of terpyridyl buffer at pH 4 (for pH > 4, the terpy ligand precipitates in solution) but also in unbuffered pure water at pH between 3 and 4.5. The electrochemical properties of **1** and **2** have been investigated in unbuffered aqueous solutions at pH 4 containing 0.1 M of supporting electrolyte such as nitrate ($NaNO_3$ or Et_4NNO_3), sulfate (K_2SO_4 or Na_2SO_4), trifluoromethanesulfonate (KCF_3SO_3 or $NaCF_3SO_3$), trifluoroacetate ($NaCF_3CO_2$), or tetrafluoroborate ($NaBF_4$). The presence of these electrolytes does not affect the stability of **2**. **1** and **2** are not soluble in the presence of perchlorate ($NaClO_4$) or hexafluorophosphate anions (KPF_6). Moreover, to stabilize the pH of solutions during exhaustive electrolyses, the electrochemical behavior of these complexes has been also studied in the presence of 0.005 M terpyridine buffer at pH 4 containing 0.1 M Na_2SO_4. At a vitreous carbon electrode, the nonelectroactivity of the aqueous solutions are in the range −0.5 to 1.3 V vs Ag/AgCl/3M KCl.

A. Electrochemical Behavior of $[Mn_2^{III,IV}O_2(terpy)_2(H_2O)_2](NO_3)_3{\cdot}6H_2O$ (2). In a preliminary work,[19] we have shown that the cyclic voltammogram (CV) of **2** in H_2O containing 0.1 M $NaNO_3$ exhibits a well-defined irreversible reduction peak at 0.64 V vs Ag/AgCl/3 M KCl and a poorly defined oxidation system characterized by a shoulder located at around 1.10 V. The shape of these later electrochemical signals strongly depends on the nature of the supporting electrolyte probably because of some adsorption phenomena at the working electrode surface. Figures 1 and S1 show the CVs of **2** in the presence of 0.1 M KCF_3SO_3 and $NaBF_4$, respectively.

Table 1 summarizes the redox potentials of **2** in aqueous solutions containing 0.1 M of the different supporting electrolytes. In 0.1 M $CF_3SO_3^-$, the irreversible reduction peak at $Ep_c^{1\prime}$ = 0.64 V (Figure 1A) is well-defined as in 0.1 M NO_3^-. A poor resolution of this peak is observed in the presence of other

(22) Chen, H.; Faller, J. W.; Crabtree, R. H.; Brudvig, G. W. *J. Am. Chem. Soc.* **2004**, *126*, 7345.

(23) Collomb Dunand-Sauthier, M.-N.; Deronzier, A.; Pradon, X.; Menage, S.; Philouze, C. *J. Am. Chem. Soc.* **1997**, *119*, 3173.

(24) Collomb Dunand-Sauthier, M.-N.; Deronzier, A.; Piron, A.; Pradon, X.; Menage, S. *J. Am. Chem. Soc.* **1998**, *120*, 5373.

(25) Collomb Dunand-Sauthier, M.-N.; Deronzier, A.; Piron. A. *J. Electroanal. Chem.* **1999**, *463*, 119.

Table 1. Electrochemical Data of **1**, **2**, and **4** in H_2O Containing 0.1 M Supporting Electrolytes (Anions BF_4^-, $CF_3SO_3^-$, NO_3^-, $CF_3CO_2^-$, or SO_4^{2-}), $v = 20$ mV s^{-1}

$[Mn_2^{III,IV}O_2(terpy)_2(H_2O)_2]^{3+}$ (**2**)	$E_{1/2}^1$, (Ep_a^1; Ep_c^1)/V $Mn_2^{III,IV}O_2 \rightleftharpoons$ $Mn_2^{IV,IV}O_2 \rightarrow Mn_4^{IV}O_5$	$Ep_c^{1'}$/V $Mn_2^{III,IV}O_2 \rightleftharpoons$ $Mn_2^{III,III}O_2 \rightarrow Mn^{II}$
BF_4^-	1.05 (1.09; 0.99)	0.41−0.52
$CF_3SO_3^-$	1.05 (1.11; 1.00)	0.64
NO_3^-	- (1.10[a]; 1.02)	0.53−0.64
$CF_3CO_2^-$	1.04 (1.10; 0.99)	0.64
SO_4^{2-}	- (1.05[a]; 0.95)	0.58

	Ep_a^3/V $Mn^{II} \rightleftharpoons Mn^{III} \rightarrow Mn_2^{III,IV}O_2$
$[Mn^{II}(terpy)_2]^{2+}$ (**1**)	0.87[a]

$[Mn_4^{IV}O_5(terpy)_4(H_2O)_2]^{6+}$ (**4**)[b]	Ep_c^2/V $Mn_4^{IV}O_5 \rightarrow Mn_2^{III,IV}O_2$
BF_4^-	0.91
$CF_3SO_3^-$	0.89
NO_3^-	0.82
$CF_3CO_2^-$	0.82−0.86
SO_4^{2-}	0.82

[a] Shoulder. [b] The H_2O ligands of **4** can be substituted by anions present in solution.

electrolytes such as BF_4^- (Figure S1) and SO_4^{2-} that appears generally at a less positive potential (from 0.58 to 0.41 V, Table 1). This reduction peak leads to the formation of the mononuclear complex **1** as the final product. The formation of **1**, on the time scale of the CV, is clearly evidenced in 0.1 M $CF_3SO_3^-$ (Figure 1A) by the presence on the positive reverse scan, of a low intensity irreversible oxidation peak at $Ep_a^3 = 0.87$ V, typical of the oxidation of this complex (see section I.C).

On the other hand, as in 0.1 M NO_3^-, the shape of the oxidation system of **2** remains poorly defined in the presence of anions such as $CF_3CO_2^-$ and SO_4^{2-}. In contrast, with 0.1 M $CF_3SO_3^-$ or BF_4^- (Figures 1A, B and S1), a partially reversible one-electron wave is clearly observed at $E_{1/2}^1 = 1.05$ V. This wave has been nonambiguously assigned to a one-electron exchange process by comparison of the $[Mn_2^{III,IV}O_2(L)_4]^{3+}$ oxidation wave[23−25] which exhibits a close intensity in the same experimental conditions and corresponds to the $Mn_2^{III,IV}O_2/Mn_2^{IV,IV}O_2$ redox couple. This is confirmed by exhaustive electrolysis experiments (see further in the text). The reversibility of the oxidation wave of **2** increases with the scan rate (Figure 1A, B and S1). In parallel, on the reverse scan, a new cathodic peak, p_c^2, appears at a less positive potential ($Ep_c^2 = 0.89$ V (Figure 1A, B) and 0.91 V (Figure S1)), and its intensity decreases as the scan rate increases. A similar behavior is observed in H_2O containing 0.1 M NO_3^-, $CF_3CO_2^-$, and SO_4^{2-} although the oxidation wave appears less defined. These observations indicate that the one-electron oxidized form of **2**, $[Mn_2^{IV,IV}O_2(terpy)_2(H_2O)_2]^{4+}$, is only moderately stable and is chemically transformed into a new species that is reduced at a slightly less positive potential (reduction peak p_c^2).

To fully characterize the respective final products issued from the oxidation and the reduction of **2**, exhaustive electrolyses have been carried out. Controlled potential electrolyses at 1.20 V of **2** aqueous solutions, whatever the electrolyte is, corroborate the instability of the $[Mn_2^{IV,IV}O_2(terpy)_2(H_2O)_2]^{2+}$ species. After the consumption of about 2−3 electrons per molecule of **2**, the current is almost equal to zero (in the presence of 0.1 M BF_4^-,

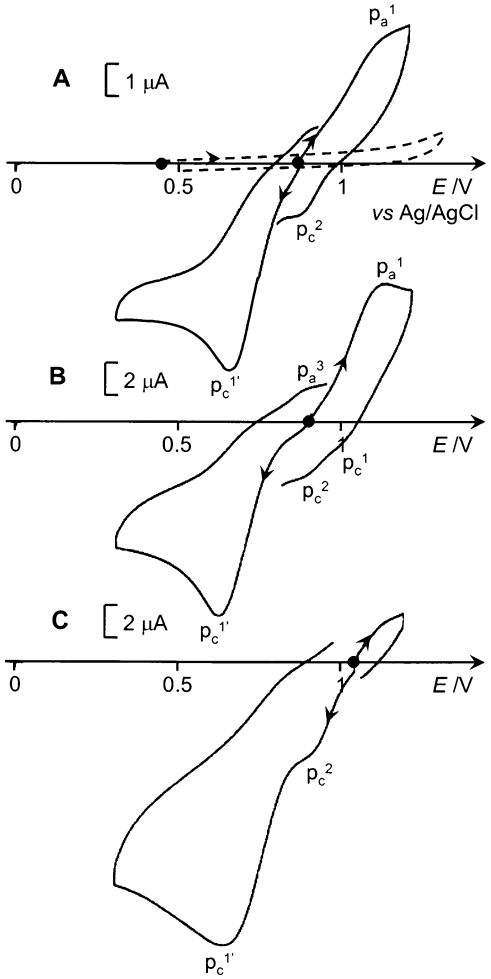

Figure 1. Cyclic voltammograms at a vitreous carbon electrode (3 mm of diameter) in H_2O + 0.1 M KCF_3SO_3 at pH 4 of (A) (- - -) electrolytic solution and (—) 2.6 mM $[Mn_2^{III,IV}O_2(terpy)_2(H_2O)_2]^{3+}$ (**2**), sweep rate $v = 5$ mV s^{-1}, (B) $v = 20$ mV s^{-1}, and (C) after exhaustive oxidation at 1.20 V, $v = 20$ mV s^{-1} (consumption of 2.75 electrons per initial molecule of **2**).

the exhaustive oxidation requires 5 electrons) and a pronounced color change of the solution from green to red is observed. The CVs recorded at the end of the electrolyses show the disappearance of the partially reversible oxidation wave at $E_{1/2}^1 = 1.05$ V, and the increase in intensity of the irreversible reduction peak p_c^2 while the irreversible peak at $p_c^{1'}$ persists (Figures 1C and S1, Table 1). This red oxidized species has been identified as the tetranuclear complex **4**, with a linear Mn_4O_5 core as demonstrated below.

Equation 2a summarizes the overall process of the electrochemical oxidation of **2**:

$$2\,[Mn_2^{III,IV}O_2(terpy)_2(H_2O)_2]^{3+} \underset{b}{\overset{a}{\rightleftharpoons}} [Mn_4^{IV}O_5(terpy)_4(H_2O)_2]^{6+} + 2\,H^+ + H_2O + 2\,e^- \quad (2)$$

It appears that the electro-oxidation of **2** leads to the aggregation of two electrogenerated $[Mn_2^{IV,IV}O_2(terpy)_2(H_2O)_2]^{4+}$ species (Scheme 2(b, c)) and not to the formation of a species containing a terminal oxo group. The aggregation involves the formation of one bridging μ-oxo anion between two $[Mn_2^{IV,IV}O_2(terpy)_2(H_2O)_2]^{4+}$ species (eq 2). The oxo bridge results from one H_2O ligand deprotonation. Obviously one or two terminal aqua group

Scheme 2. Interconversion for Mono- (**1**), Bi- (**2**, **3**), and Tetranuclear (**4**) Terpyridine Complexes in Aqueous Solutions (E = Electrochemical Step, C = Chemical Step)

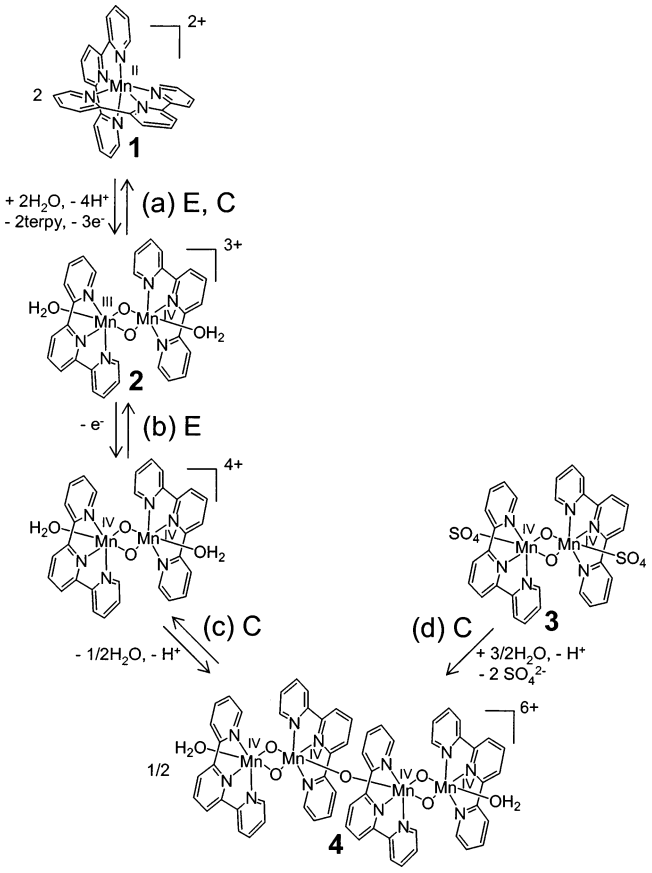

of **4** can be substituted by anions coming from the electrolyte. This phenomenon has been neglected in eq 2 for simplification.

Electrochemical and spectroscopic characteristics of these resulting oxidized solutions are identical to those of an authentic sample of **4**, prepared as described in ref 22, in the same media. For example, in H_2O containing 0.1 M KCF_3SO_3, the CV of **4** between 0 and 1.3 V shows only two successive irreversible reduction peaks located at $Ep_c^2 = 0.89$ V and $Ep_c^{1'} = 0.64$ V, corresponding, respectively, to the reduction of **4** into **2** and to the reduction of **2**, formed at the time scale of the CV, into **1** (Figure S2). As indicated in Table 1, the reduction potential of **4** is not exactly the same according to the nature of the anions (comprised between 0.82 and 0.91 V). However, due to the strong adsorption phenomena at the working electrode observed during the CV recording, this shift in potential cannot be considered as proof of the substitution of the H_2O ligands of **4** by anions present in solution as supporting electrolytes.

The **2** oxidized solutions are stable for several hours. Their X-band EPR spectra recorded between 4 and 170 K consist of a very weak 16-line signal corresponding to a small amount of **2** remaining in solution. This is consistent with the formation of the EPR silent complex **4**.[22]

Figure 2 illustrates the UV−visible absorption spectra changes during the electrochemical oxidation of a 2 mM solution of **2** in H_2O containing 0.1 M Na_2SO_4. The initial spectrum of the green solution shows the expected four bands located at 275, 330, 553, and 654 nm (Figure 2A(a) and 2B(a)). The absorptions between 380 and 500 nm are ascribed to contributions of d−d transitions of the Mn^{IV} ion and metal to ligand charge-transfer

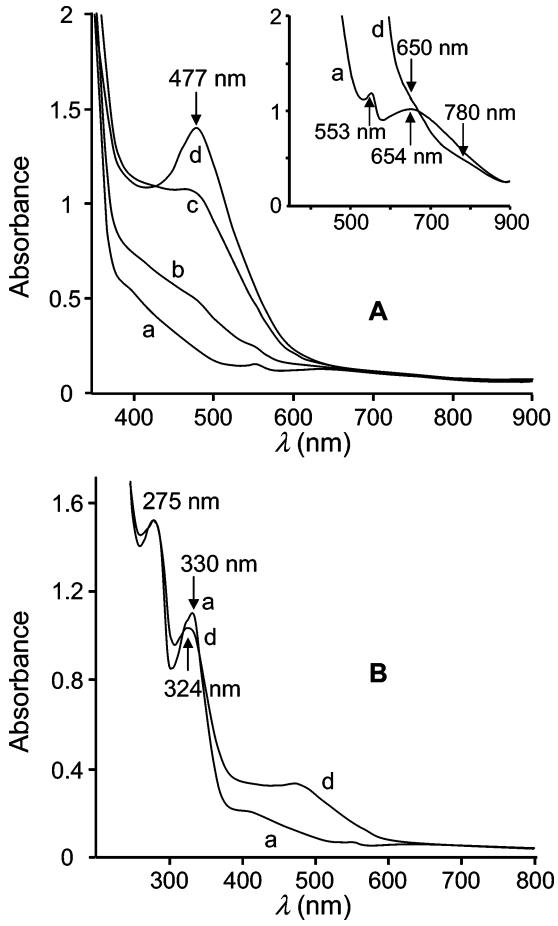

Figure 2. UV−visible absorption spectra changes during electrolysis of a 2 mM solution of **2** in H_2O + 0.1 M Na_2SO_4: (A) (a) initial solution; (b) after oxidation of (a) at 1.20 V (0.5 electron consumed per molecule of **2**); (c) 1.3 electrons; (d) 3 electrons; $l = 1$ mm; insert: solution (a) and (d) with $l = 1$ cm. (B) (a) and (d) diluted solutions (A)(a) and (A)(d), respectively; $l = 1$ mm.

(MLCT) bands from oxo ligands to Mn^{IV} ion. The band located at 553 nm corresponds to a d−d transition of Mn^{IV} ion, and that at 654 nm can be ascribable to an MLCT band of the oxo to the Mn^{IV} ion.[19,26] Identical spectra are obtained in the presence of the different supporting electrolytes suggesting that the labile H_2O ligands of **2** are not replaced by anions but remain coordinated to the manganese ions. During the electrolysis at 1.20 V, a new intense visible band appears progressively at 477 nm (Figure 2A(a−d)). This band, responsible for the red color of the solution, can be assigned to the contributions of Mn^{IV} d−d transitions and an MLCT band of oxo ligands to Mn^{IV}. The final absorption spectrum (Figure 2A(d) and 2B(d)) presents three bands at 275, 324, and 477 nm and two shoulders at 650 and 780 nm. This spectrum is closely superimposable with that of a chemical sample of **4** (1 mM) in the same electrolyte, which demonstrates that the transformation is quasi-quantitative. In the presence of other electrolytes, the spectra are similar, except that the λ_{max} value of the visible band slightly varies (λ_{max} = 473 nm (BF_4^-), 478 ($CF_3SO_3^-$), 478 (NO_3^-), 475 ($CF_3CO_2^-$), and 477 (SO_4^{2-}) for 2 mM initial solutions of **2**). This indicates either a substitution of some H_2O ligands of **4** by anions or the formation of ion pairs between the hexacationic species **4** and

(26) Gamelin, D. R.; Kirk, M. L.; Stemmler, T. L.; Pal, S.; Armstrong, W. H.; Penner-Hahn, J. E.; Solomon, E. I. *J. Am. Chem. Soc.* **1994**, *116*, 2392.

the anions of the electrolyte (see section II.A). It should be noted that the absorption spectra of **4** are also close to those of $[Mn_4^{IV}O_6(L)_6]^{4+}$ (L= bpy or phen) that present equally an intense band at 425 nm (Mn^{IV} d−d transitions) and two shoulders at 670 and 780 nm.[23−25]

Moreover, a comparison of the initial and fully oxidized solutions absorption spectra in the UV region (Figure 2B) indicates that the oxidation of **2** and the following chemical reaction does not lead to release of terpy ligand in solution. Indeed, the UV band at 275 nm is not shifted after oxidation, whereas that located at 330 nm is slightly shifted to 324 nm. In addition, the intensity of these two UV absorption bands is similar for the two spectra, in accordance with two compounds structurally related and with the quantitative formation of **4**.

It should be recalled that, theoretically, the formation of a Mn^{IV} species by electrochemical oxidation of **2** involves the exchange of only one electron per molecule (eq 2a). Experimentally, as previously observed for the electrochemical oxidation of $[Mn_2^{III,IV}O_2(L)_4]^{3+}$ in aqueous solutions, for instance, two to five electrons are required to oxidized a 2 mM solution of **2**. The observed excess of coulometry is due to a slow, competitive direct oxidation of the electrolyte or water at this potential as it has been established by separate experiments conducted in the absence of **2**. The excess of coulometry observed depends also on the initial concentration of the complex as well as the nature of the supporting electrolyte. It is larger when BF_4^- is used compared to $CF_3SO_3^-$, SO_4^{2-}, and NO_3^- and increases when the concentration of **2** is lower than 2 mM.

At the end of the electrolyses of 2 mM solutions of **2**, the pH is about equal to 2.6. The decrease of the pH (initially of 4) indicates the release of protons in solution. This can be attributed to the competitive oxidation of water (a decrease of pH is also observed after electrolyses conducted in the absence of dimer) and, in addition, to the formation of oxo bridges between two or several $[Mn_2^{IV,IV}O_2(terpy)_2(H_2O)_2]^{4+}$ dimers. As will be discussed in detail in section II, a decrease of pH is also observed when **3** is dissolved in aqueous solutions.

By another way, the reduction of **4** returns back to **2**, as attested by the presence on the CV of the irreversible peak $p_c^{1'}$ of **2** that follows p_c^2 (Figures 1C and S1). This assumption has been verified by a controlled-potential reduction of the oxidized red solution at 0.85 V. As judged by the electrochemical and spectroscopic analysis of the solution, **2** is quantitatively restored after the consumption of only one electron per initial molecule of **2** regardless of the anion used as electrolyte (eq 2b).

All these results are evidence that the electrochemical behavior of **2** is basically the similar to that of $[Mn_2^{III,IV}O_2(L)_4]^{3+}$ (L = bpy and phen), the main difference being the markedly lower stability of the corresponding $Mn_2^{IV,IV}O_2$ species in the case of **2** due to a faster evolution into a tetranuclear species. Indeed, at the same scan rate, the redox system $Mn_2^{III,IV}O_2/Mn_2^{IV,IV}O_2$ appears much less reversible for the terpy complex than those of the bpy and phen ones and at a less positive potential ($E_{1/2}$ = 1.05 V (terpy), 1.16 V (bpy), and 1.15 V (phen)).[23−25] These differences can be explained by the kinetics of the dimerization process following the one-electron oxidation of the $Mn_2^{III,IV}$ species, which is faster in the case of the terpy complex. Indeed, the dimerization process of $[Mn_2^{IV,IV}O_2(L)_4]^{4+}$ (Scheme 1) requires the decoordination of one L ligand per binuclear and the formation of two oxo bridges. In the case of **2** (Scheme 2(c)), the aggregation of $[Mn_2^{IV,IV}O_2(terpy)_2(H_2O)_2]^{4+}$ to form **4** should be easier and faster since the process does not need a decoordination of a terpy ligand and involves the formation of only one oxo bridge between two binuclear entities. In addition, the formation of this oxo bridge is facilitated because the $[Mn_2^{IV,IV}O_2(terpy)_2(H_2O)_2]^{4+}$ species already contains aqua groups in its coordination sphere. In a similar way, the easier reduction of **4** (Ep_c^2 = 0.82−0.91 V, Table 1) compared to $[Mn_4^{IV}O_6(L)_6]^{4+}$ (Ep_c = 0.40 V (bpy) and 0.48 V (phen)) should be due to, as well as in the case of their formation, the difference in terms of kinetics of the chemical reactions coupled to the electron transfer. Indeed, in the case of **4**, the electrochemical regeneration of **2** implies only a double protonation of the mono-μ-oxo-bridge, while, for $[Mn_4^{IV}O_6(L)_6]^{4+}$, a double protonation of two μ-oxo-bridges and a coordination of one L ligand per dimer are required. In addition, **4** is quantitatively reduced into **2** by an exhaustive reduction at controlled potential, and this reduction involves only one-electron per molecule of dimeric unit formed. In the case of the bpy and phen complexes, since $[Mn_2^{III,IV}O_2(L)_4]^{3+}$ and $[Mn_4^{IV}O_6(L)_6]^{4+}$ complexes are irreversibly reduced at similar potentials (about 0.4 V), the $[Mn_2^{III,IV}O_2(L)_4]^{3+}$ complexes cannot be regenerated selectively by electroreduction of $[Mn_4^{IV}O_6(L)_6]^{4+}$.[23−25]

Controlled-potential exhaustive reductions at 0.55 V of 2 mM solutions of **2** in H_2O, containing 0.1 M of either NO_3^-, SO_4^{2-}, or $CF_3SO_3^-$ anions, consume one electron per molecule of **2**. In 0.1 M NO_3^- or SO_4^{2-} the electrochemical and spectroscopic features of the reduced yellow solutions are identical to those obtained from a chemical sample of **1** in the same media (see section I.C). In the presence of $CF_3SO_3^-$, the electrogenerated complex **1** precipitates in solution. The CVs of the reduced solutions in NO_3^- or SO_4^{2-} show mainly an irreversible (broad) oxidation peak around Ep_a^3 = 0.87 V assigned to the Mn^{II}/Mn^{III} redox couple of **1**. The formation of this complex is confirmed by the absorption spectrum of the electroreduced solution that shows the five characteristic UV−visible bands of **1** at 265, 275, 283, 322, and 334 nm (Figure S3). The amount of **1** formed is estimated to 2 mM using the ϵ values of those bands determined from a chemical sample of **1**. An insoluble brown side product is also formed in solution during the electrolyses and probably corresponds to an undefined manganese oxide species, noted $(Mn^{IV}O_2)_x$ as observed during the electroreduction of the $[Mn_2^{III,IV}O_2(L)_4]^{3+}$ (L = bpy; dmbpy) and $[Mn_2^{III,IV}O_2(terpy)_2(CF_3CO_2)_2]^+$ complexes in CH_3CN.[27,28] These results show that the initially formed $[Mn_2^{III,III}O_2(terpy)_2(H_2O)_2]^{2+}$ species is unstable and disproportionates to Mn^{II} and Mn^{IV} species (eq 3).

$$[Mn_2^{III,IV}O_2(terpy)_2(H_2O)_2]^{3+} + e^- \underset{b}{\overset{a}{\rightleftarrows}} [Mn^{II}(terpy)_2]^{2+} + (Mn^{IV}O_2)_x + 2\,H_2O \quad (3)$$

The brown precipitate is not redissolved during reoxidation of the solutions at 0.80 V, and as a consequence, only 48% of **2** is restored. The pH of the unbuffered aqueous solutions slightly

(27) Collomb-Dunand-Sauthier, M.-N.; Deronzier, A. *J. Electroanal. Chem.* **1997**, *428*, 65.
(28) Baffert, C.; Collomb, M.-N.; Deronzier, A.; Pécaut, J.; Limburg, J.; Crabtree, R. H.; Brudvig, G. W. *Inorg. Chem.* **2002**, *41*, 1404.

changes during these sequential electrolyses. It increases from 3.7 to 5.3 after the exhaustive reduction and returns to 3.6 after the exhaustive reoxidation.

B. Electrochemical Behavior of 2 in Aqueous terpy/terpyH$^+$ Buffered Medium (pH 4). The CVs of **2** in an aqueous 0.005 M terpy/terpyH$^+$ buffered solution containing 0.1 M Na_2SO_4 appear poorly defined due to the strong adsorption at the working electrode surface of the uncomplexed terpy ligand. Controlled potential reduction and oxidation of **2** in this solvent lead also to the formation of **1** and **4**, respectively. **1** is produced quantitatively by an exhaustive reduction at 0.20 V (2.8 electrons consumed per molecule of **2**) due to the presence of free terpy ligands in the solution (eq 4a).

$$[Mn_2^{III,IV}O_2(terpy)_2(H_2O)_2]^{3+} + 2\ terpy + 4\ H^+ + 3\ e^- \underset{b}{\overset{a}{\rightleftarrows}} 2\ [Mn^{II}(terpy)_2]^{2+} + 4\ H_2O \quad (4)$$

The overall chemical process is obviously reversible as demonstrated by a subsequent oxidation of the reduced solution at 1.00 V (three electrons consumed per initial molecule of **2**) that restores quantitatively **2** (eq 4b). **4** is also quantitatively obtained by an exhaustive oxidation of **2** at 1.20 V. The visible absorption spectrum of the fully oxidized solution is identical to those obtained in nonbuffered solutions with an intense visible band located at 477 nm and two shoulders at 650 and 780 nm. The initial solution pH of 4 decreases to 3.7 after oxidation and increases to 4.3 after reduction. The relative stabilization of the pH of the aqueous solution during electrolyses and the presence of an excess of terpy do not prevent the formation of **4**.

C. Electrochemical Behavior of [Mn^{II}(terpy)$_2$]$^{2+}$ (1) in Aqueous Solutions. 1 can be formed in situ by simple mixing of 2 equiv of terpy ligand with 1 equiv of Mn^{2+} cation in H_2O at pH 4 containing 0.1 M $NaNO_3$ or Na_2SO_4 (**1** is poorly soluble in the presence of $CF_3SO_3^-$). The visible absorption spectrum of the yellow pale solution (not shown), as well as its CV, is identical to a synthetic sample of **1** in the same electrolytes. Figure 3 shows the CV of **1** that exhibits no reduction peak but a broad oxidation peak around $Ep_a^3 = 0.87$ V (shoulder) corresponding to the metal oxidation process Mn^{II}/Mn^{III}. The irreversibility of this oxidation process is due to the formation of **2**. This is evidenced, on the CV time scale, by the presence of the shoulder at 1.10 V, typical of the oxidation of **2** and, on the reverse scan, by the presence of the two irreversible peaks at $Ep_c^2 = 0.86$ and $Ep_c^{1'} = 0.57$ V corresponding to the reduction of its oxidized product (**4**) and to its reduction into **1**, respectively. A controlled-potential oxidation of a 1 mM solution of **1** at 0.85 V consumes 1.5 electrons per initial molecule of **1** and furnishes a green solution that exhibits the spectroscopic and electrochemical characteristics of a solution of **2** (Figures 3 and 4). The amount of **2** is estimated to 0.48 mM (yield 96%) using the ϵ value (585 M^{-1} cm^{-1}) of its visible absorption band at $\lambda_{max} = 653$ nm. The reaction mechanism for the formation of **2** is probably similar to that proposed for the formation of $[Mn_2^{III,IV}O_2(L)_4]^{3+}$ in CH_3CN[29] or in H_2O[23−25] from electrochemical oxidations of the corresponding $[Mn^{II}(L)_3]^{2+}$ complexes. The process involves the disproportionation of the unstable one-electron oxidized form of **1**, $[Mn^{III}(terpy)_2]^{3+}$ to

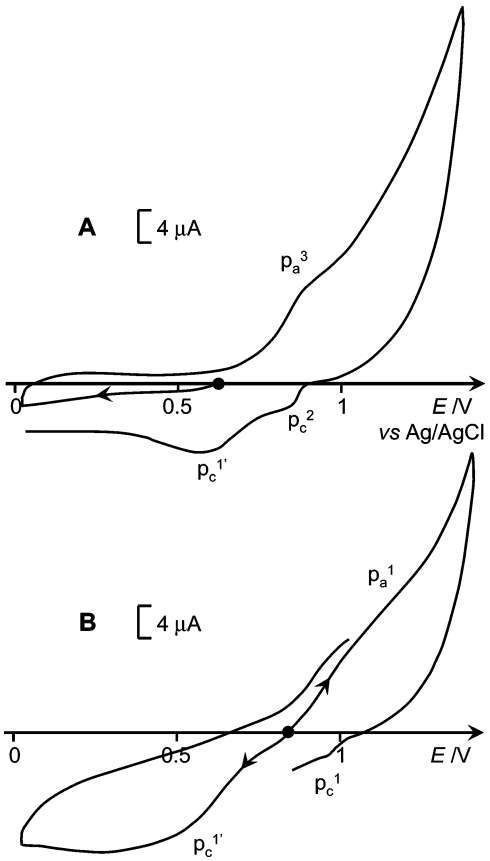

Figure 3. Cyclic voltammograms in H_2O + 0.1 M Na_2SO_4 (pH = 4) at a vitreous carbon electrode (diameter 5 mm) of (A) 1 mM $[Mn^{II}(terpy)_2]^{2+}$ (**1**), (B) after exhaustive oxidation at 0.85 V; $v = 20$ mV s^{-1}.

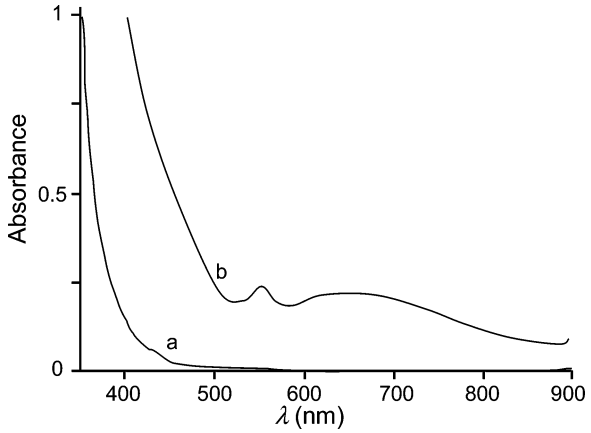

Figure 4. Visible absorption spectra of a 1 mM solution of **1** in H_2O + 0.1 M Na_2SO_4 (pH = 4): (a) initial solution; (b) after exhaustive oxidation of (a) at 0.85 V (1.5 electrons consumed per molecule of **1**).

Mn^{II} and Mn^{IV} species. The Mn^{IV} formed probably reacts with another Mn^{III} to form the di-μ-oxo $Mn_2^{III,IV}$ species via release of one terpy ligand, and interaction with water (eq 5, Scheme 2(a)).

$$2\ [Mn^{II}(terpy)_2]^{2+} + 2\ H_2O \underset{b}{\overset{a}{\rightleftarrows}} [Mn_2^{III,IV}O_2(terpy)_2(H_2O)_2]^{3+} + 2\ terpy + 4\ H^+ + 3\ e^- \quad (5)$$

This oxidation at 0.85 V induces only a weak decrease of the pH of the solution (4 to 3.78) because the protons release during the reduction partially protonate the terpy ligand. The presence

(29) Morrison, M. M.; Sawyer, D. T. *Inorg. Chem.* **1978**, *17*, 333.

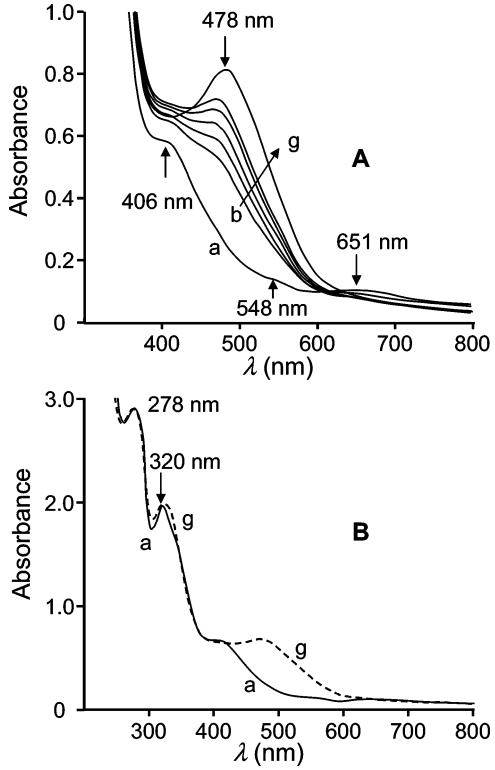

Figure 5. Time resolved UV−visible absorption spectra of 1.2 mM $[Mn_2^{IV,IV}O_2(terpy)_2(SO_4)_2]$ (**3**) in H_2O + 0.1 M Na_2SO_4 during the formation of **4**: (A) initial solution after (a) 5 min; (b) 15 min; (c) 20 min; (d) 25 min; (e) 35 min; (f) 1 h 10 min; (g) 2 h with l = 1 mm. (B)(a) and (g), solutions (A)(a) and (g), respectively; l = 1mm.

of terpy ligand in solution and, in addition, 0.1 M SO_4^{2-} anions as supporting electrolytes are responsible of the poor resolution of the CV of **2** (Figure 3B). Obviously, **4** can be quantitatively generated by a further oxidation at 1.25 V of the oxidized solution of **2** or by a direct oxidation of a solution of **1** at 1.25 V.

The dimerization reaction (eq 5a) is an overall reversible process. A subsequent controlled potential reduction at 0.45 V of the electrogenerated solution of **2** restores entirely the initial amount of **1** after the consumption of three electrons per molecule of **2** (eq 5b).

II. Dissolution of $[Mn_2^{IV,IV}O_2(terpy)_2(SO_4)_2]\cdot 3H_2O$ (3) in Aqueous Solutions. **3** is only poorly soluble in water, and its dissolution is improved starting from crystals carefully ground. Dark-green solutions of **3** in pure water or in the presence of 0.1 M supporting electrolytes (anions NO_3^-, SO_4^{2-}, $CF_3SO_3^-$, $CF_3CO_2^-$, or BF_4^-) are only stable a few minutes and then lead progressively to red solutions showing similar spectroscopic and electrochemical characteristics to those obtained by an electrochemical oxidation of **2**. These observations show that **3** is spontaneously converted into **4** in aqueous solutions (Scheme 2(d)). Equation 6 summarizes the global process knowing that it is possible that some SO_4^{2-} anions remain coordinated to the manganese in terminal positions or that other electrolyte anions substitute the aqua ligands:

$$2\,[Mn_2^{IV,IV}O_2(terpy)_2(SO_4)_2] + 3\,H_2O \rightarrow [Mn_4^{IV}O_5(terpy)_4(H_2O)_2]^{6+} + 2\,H^+ + 4\,SO_4^{2-} \quad (6)$$

Figure 5 illustrates the UV−visible absorption spectral changes of a 1.2 mM solution of **3** in H_2O containing 0.1 M Na_2SO_4 over 2 h. The entire dissolution of **3** is achieved after 5 min. The absorption spectrum of **3** shows then two UV bands at 278 and 320 nm, three shoulders at 340, 406, and 548 nm and one visible band at 651 nm as previously observed.[20,22] After 5 min, the formation of **4** is evidenced by the progressive increase of the visible absorption band at 478 nm to the detriment of that at 651 nm and the shift of the band at 320 to 324 nm. The maximum absorption of the band at 478 nm is reached after about 2 h under stirring, and almost no change of intensity is obtained after several hours as for the electrogenerated species. The similarity of this final UV−visible spectrum to those obtained by an electrochemical oxidation of **2** or by the dissolution of a chemical sample of **4** at 0.6 mM attests the quantitative formation of **4**.

A. Effects of the Concentration of 3 and of the Presence of Anions on the Visible Absorption Band of 4. To estimate the effect of the complex concentration and the influence of the nature of the anions present in solution on the shift of the visible absorption band located around 478 nm of **4**, **3** has been dissolved at concentrations comprised between 1 and 5 mM in pure water or in the presence of NO_3^-, SO_4^-, or $CF_3SO_3^-$ at 0.1 M. The formation of **4** has been followed by UV−visible absorption spectroscopy. Figure S4 exhibits the final spectra obtained in these different conditions. In all cases, **4** is quantitatively formed. The intensity of the visible band is well proportional to the quantity of **3** dissolved in all the media studied. It can also be noticed that when the concentration of the complex increases, the resolution of this visible band is improved and its λ_{max} is shifted toward a higher wavelength. In addition, the nature of the anions present in solution affects the λ_{max} value. For instance, at 5 mM concentrations, the λ_{max} values obtained are comprised between 474 and 482 nm. Moreover, addition of anions such as NO_3^- or $CF_3SO_3^-$ (0.1 M) to a solution of **4** in pure water (obtained by dissolution of 5 mM solution of **3**) leads to a rapid shift (few seconds) of the λ_{max} located at 474 nm toward 482 and 478 nm, respectively. These results clearly show that the anions present in solution interfere with **4**, by formation of ion pairing and/or by the substitution of some anions to the peripheral metals of **4**.

The formation of **4** from **3** is accompanied by the release of one proton, and, at least, of one SO_4^{2-} per **2** (eq 6). Experimentally we observe a pH decrease during the formation of **4**. This pH decrease is also well proportional to the initial concentration of **3** (ranging from 1 to 9 mM). For each concentration, after the quantitative formation of **4**, the number of protons released is close to unity per one **3** dimer in accordance with the formation of the tetranuclear species. These results are in accordance with the fact that no change of pH is observed after dissolution of a chemical sample of **4** at different concentrations (from 0.25 to 1 mM) in water containing 0.1 M supporting electrolyte such as NO_3^- or SO_4^{2-}.

As expected, all solutions exhibit no EPR signal.

B. Electrochemical Properties of $[Mn_2^{IV,IV}O_2(terpy)_2(SO_4)_2]$ (3) in Aqueous Solution. The formation of **4** has also been followed by electrochemistry. The CV of the initial solution of **3** in H_2O containing 0.1 M KCF_3SO_3 shows only one irreversible reduction peak at Ep_c = 0.66 V showing that **3** is reduced at a potential close to that of **2** (Figure 6A).

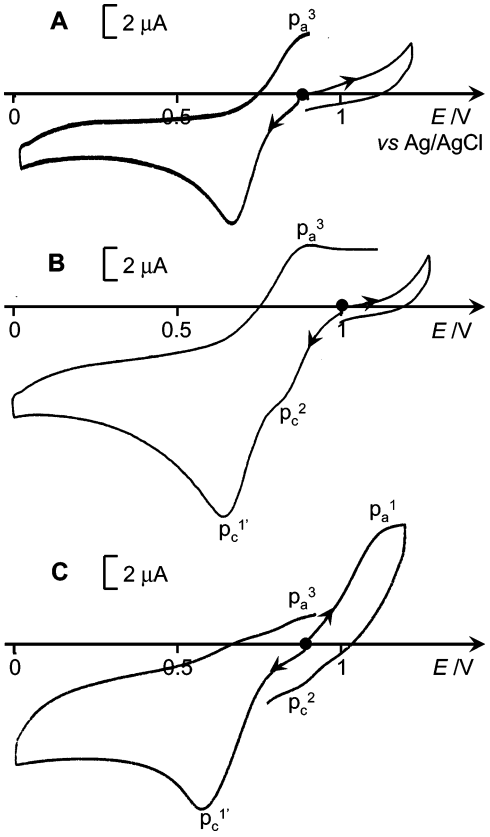

Figure 6. Cyclic voltammograms at a vitreous carbon electrode (3 mm of diameter) in H_2O + 0.1 M KCF_3SO_3 of (A) 1.2 mM of $[Mn_2^{IV,IV}O_2(terpy)_2(SO_4)_2]$ (**3**), (B) after 2 h (quantitative formation of **4**) and (C) after exhaustive reduction of (B) at 0.90 V (quantitative formation of **2**), $v = 50$ mV s^{-1}.

After 5 min, the appearance and the progressive increase of a reduction peak at $Ep_c^2 = 0.86$ V corresponding to the formation of **4**, followed by the reduction peak at $Ep_c^1 = 0.64$ V of **2** (issued from the initial reduction of **4**), is observed. After 2 h, the transformation into **4** is total (Figure 6B), and the CV obtained is similar to that obtained by electrochemical oxidation of **2** with two irreversible peaks at $Ep_c^2 = 0.86$ V and $Ep_c^1 = 0.64$ V. The reduction of **4** into **2** is confirmed by a 0.9 V electrolysis that consumes 0.75 electron and furnishes **2** quantitatively (Figure 6C, eq 2b).

C. ESI Mass Spectrometry. Figure 7 shows the ESI-MS spectra obtained in positive mode immediately after the dissolution of **3** in pure water and after the entire formation of **4**. Characteristic peaks of both complexes have been obtained. These two compounds are only detected in water without addition of electrolyte. The spectrum of the neutral **3** complex shows three main peaks in the 650−1000 area, at $m/z = 703.9$, 721.0, and 800.9, respectively, assigned to the monocationic species $[Mn_2^{III,IV}O_2(terpy)_2(SO_4)]^+$, $[Mn_2^{IV,IV}O_2(terpy)_2(SO_4)(OH)]^+$, and $[Mn_2^{IV,IV}O_2(terpy)_2(SO_4)_2(H)]^+$ in comparison with the isotopic profiles calculated for these formulas. The mass spectrum of **4** has been recorded in the same experimental conditions to that of **3** and shows a new peak at $m/z = 712.0$ corresponding to a doubly charged ion, assigned to the tetranuclear compound $[Mn_4^{IV}O_5(terpy)_4(SO_4)_2]^{2+}$. The peak at 800.9 has disappeared, while the two peaks at 703.9 and 721.0 are always present. The respective intensities of these two last peaks are different for **3** and **4** mass spectra. A possible explanation is that these two monosulfate species have not the same origin, and in the case of the **4** spectrum, they should arise from the break of the tetranuclear complex in the spectrometer. In addition, obtaining the peak corresponding to $[Mn_4^{IV}O_5(terpy)_4$-

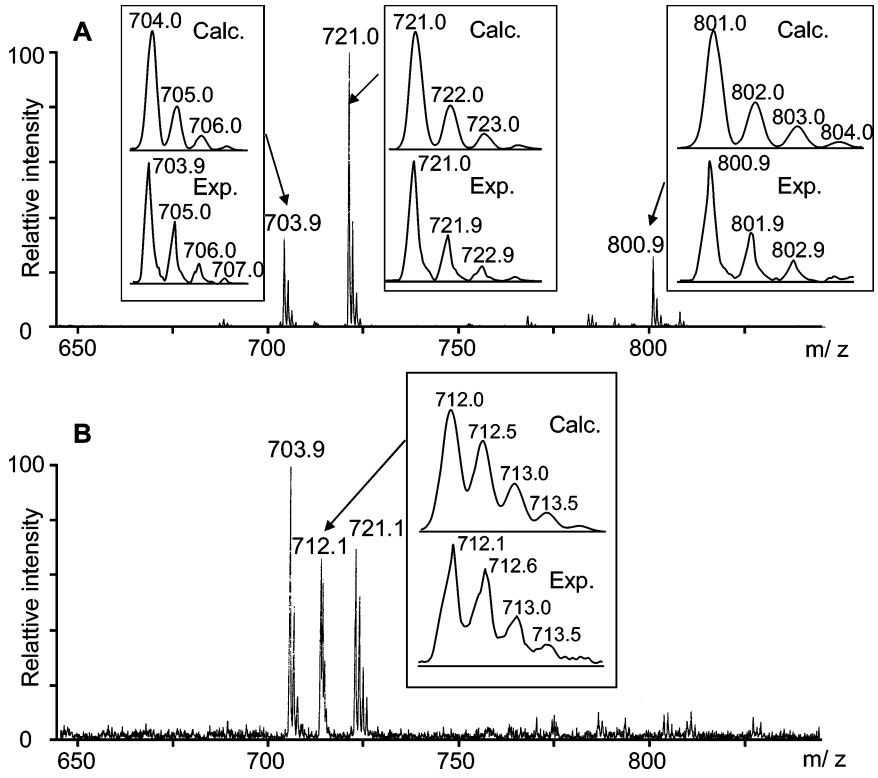

Figure 7. ESI mass spectra of (A) a 2.4 mM solution of **3** in H_2O, (B) a 3 mM solution of **3** in H_2O after its entire transformation into **4**. The peak expansions at $m/z = 703.9$, 721.0, 800.9, and 721.1 have been compared to the calculated isotopic profiles for $[Mn_2^{III,IV}O_2(terpy)_2(SO_4)]^+$ (704.0), $[Mn_2^{IV,IV}O_2(terpy)_2(SO_4)(OH)]^+$ (721.0), $[Mn_2^{IV,IV}O_2(terpy)_2(SO_4)_2(H)]^+$ (801.0), and $[Mn_4^{IV}O_5(terpy)_4(SO_4)_2]^{2+}$ (712.0).

$(SO_4)_2]^{2+}$ is not a proof of sulfate anion coordination since H_2O ligands are usually too labile to remain coordinated to manganese in electrospray ionization conditions.[30]

III. Attempts to Photoinduce the Oxidation of 2 in the Presence of $[Ru^{II}(bpy)_3]^{2+}$ in Aqueous Solution. A photoinduced oxidation of **2** in the presence of the photosensitizer $[Ru^{II}(bpy)_3]^{2+}$ in aqueous solution needs the use of a sacrificial oxidant that is irreversibly reduced allowing the net conversion of $[Ru^{II}(bpy)_3]^{2+}$ into $[Ru^{III}(bpy)_3]^{3+}$. The $[Ru^{III}(bpy)_3]^{3+}$ complex can then act as an oxidant toward **2** by an intermolecular electron transfer since the potential of the Ru^{II}/Ru^{III} redox couple in aqueous solution ($E_{1/2}$ = 1.1 V vs Ag/AgCl/KCl 3 M) is higher than that of $Mn_2^{III,IV}/Mn_2^{IV,IV}$ ($E_{1/2}{}^1$ = 1.05 V). Recently, we have demonstrated that such photoinduced processes occur at the quantitative scale with a mixture of $[Mn_2^{III,IV}O_2(L)_4]^{3+}$ (L = bpy and dmbpy) and $[Ru^{II}(bpy)_3]^{2+}$ in the presence of an excess of the 4-bromophenyl diazonium salt, ArN_2^+, playing the role of the irreversible electron acceptor in CH_3CN medium.[31] In aqueous solution diazonium salts are not stable enough to be used as a sacrificial electron aceptor. Two other irreversible electron acceptors have been then tested, commonly used in the literature to photogenerate $[Ru^{III}(bpy)_3]^{3+}$ in aqueous medium: the peroxodisulfate, $S_2O_8^{2-}$, and the pentaamine cobalt complex, $[Co(NH_3)_5Cl]^{2+}$. In the eighties, these both compounds have been largely used associated with the complex $[Ru^{II}(bpy)_3]^{2+}$ for the catalytic oxidation of water in dioxygen in the presence of heterogeneous catalysts such as RuO_x, IrO_x, and TiO_2.[32−35] $S_2O_8^{2-}$ reacts with the excited state of the ruthenium complex, $[Ru^{II}(bpy)_3]^{2+*}$, to form the $[Ru^{III}(bpy)_3]^{3+}$ species (eq 7).[32]

$$2\,[Ru(bpy)_3]^{2+*} + S_2O_8{}^{2-} \rightarrow 2\,[Ru(bpy)_3]^{3+} + 2\,SO_4{}^{2-} \quad (7)$$

Moreover, since $S_2O_8^{2-}$ does not present any visible band, no interference with the photophysical properties of the ruthenium complex is expected.

We have found that the continuous irradiation of an aqueous solution containing a mixture of $[Ru(bpy)_3]^{2+}$, $S_2O_8^{2-}$, and **2** in buffered aqueous medium ($ClAcOH/ClAcO^-$) leads to a fast O_2 evolution. However, a similar O_2 evolution has been also observed with a lower rate constant in the absence of **2**. This indicates that the presence of manganese complex is not needed to observe O_2 evolving. Moreover, under UV irradiation, it has been recently shown that $S_2O_8^{2-}$ reacts with water to form dioxygen.[36] So, this electron acceptor is not adapted since the O_2 source remains ambiguous.

Concerning $[Co^{III}(NH_3)_5Cl]^{2+}$, this irreversible electron acceptor is known to react with $[Ru(bpy)_3]^{2+*}$ following eq 8:[37−39]

$$[Ru(bpy)_3]^{2+*} + [Co^{III}(NH_3)_5Cl]^{2+} \rightarrow [Ru(bpy)_3]^{3+} + Co^{2+} + 5\,NH_3 + Cl^- \quad (8)$$

This reaction is irreversible since the cobalt(II) ion is rapidly hydrated. Nevertheless, the $[Co^{III}(NH_3)_5Cl]^+$ complex is capable of interaction by energy transfer with the excited state of the ruthenium complex because of its intense color. Moreover, its reduction releases five NH_3 molecules (eq 8) and leads to a strong increase of the basicity of the medium. That is the reason continuous irradiation of a solution containing a mixture of $[Ru(bpy)_3]^{2+}$, $[Co^{III}(NH_3)_5Cl]^{2+}$, and **2** yields a rapid degradation of the manganese complex in insoluble manganese oxide $(Mn^{IV}O_2)_x$, since **2** is stable only at a pH below 4.5 and no significant amount of O_2 is observed.

These preliminary photochemical results show that the optimum experimental conditions for a photochemical study of these systems in aqueous solutions are difficult to determine and that a good candidate for the function of irreversible electron acceptor mimicking the PSI part remains to be found. No definitive conclusion can be drawn about the capability of **2** to catalyze the oxidation of water photochemically.

Concluding Remarks

To examine the real ability of the binuclear di-μ-oxo $Mn_2^{III,IV}$ complex **2** to act as a catalyst for water oxidation, we have investigated the redox properties of the mononuclear Mn^{II} complex **1** and of **2** in aqueous solutions. The electrochemical oxidation of **1** is irreversible and leads to the quantitative formation of **2** (Scheme 2(a)). A further oxidation of **2** quantitatively yields the tetranuclear Mn^{IV} complex **4** (Scheme 2(b, c)). **4** is also formed by simple dissolution of the di-μ-oxo $Mn_2^{IV,IV}$ dimer **3**, in aqueous solution (Scheme 2(d)).The formation of these high valent polynuclear oxomanganese complexes is due to the significant tendency of Mn^{IV} species to aggregate by formation of oxo bridges. **2** and **4** can be generated selectively because the two oxidation steps are clearly separated (about 180 mV). These two transformations are chemical reversible by reduction processes. **2** can be regenerated quantitatively by reduction of **4** since the reduction potentials of these two complexes are clearly separated ($Ep_c{}^{1\prime}$ = 0.64 V for **2** and $Ep_c{}^2$ = 0.91 V for **4**). These data are evidence that the electrochemical behavior of these manganese terpy complexes is basically the similar to that of the bpy and phen parent ones previously reported. Therefore, it appears that the electrochemical oxidation of **2** in aqueous solution is only a one-electron process and leads to the stable tetranuclear complex **4** formed by a mono-μ-oxo bridge formation between two oxidized $[Mn_2^{IV,IV}O_2(terpy)_2(H_2O)_2]^{4+}$. **4** cannot be further oxidized to reach a higher oxidation state since the CV of this complex shows no oxidation wave in the potential range of the solvent. These results confirm that the redox properties of these kind of manganese complexes are radically different compared to that of the ruthenium analogous ones because, in the case of manganese complexes, the formation of oxo bridges prevent that of terminal oxo ligands.

Another evidence of this work is that **4** is stable in aqueous solutions (several hours), and even if is a good synthetic analogue of the "dimers-of-dimers" model compound of the OEC in PSII,[7] this complex is not able to oxidize water. Since **4** results from an one-electron oxidation of **2**, **2** cannot act as an efficient homogeneous electrocatalyst for water oxidation.

(30) Anderson, U. N.; McKenzie, C. T.; Bojesen, G. *Inorg. Chem.* **1995**, *34*, 1435.
(31) Baffert, C.; Dumas, S.; Chauvin, J.; Leprêtre, J.-C.; Collomb, M.-N.; Deronzier, A. *Phys. Chem. Chem. Phys.* **2005**, *7*, 202.
(32) Humphry-Baker, R.; Lilie, J.; Graetzel, M. *J. Am. Chem. Soc.* **1982**, *104*, 422.
(33) Collin, J.-P.; Lehn, J.-M.; Ziessel, R. *Nouv. J. Chim.* **1982**, *6*, 405.
(34) Lehn, J.-M.; Sauvage, J.-P.; Ziessel, R. *Nouv. J. Chim.* **1980**, *4*, 355.
(35) Shafirovich, V. Y.; Strelets, V. V. *Nouv. J. Chim.* **1982**, *6*, 183.
(36) Nagashima, K.; Inoue, M.; Namiki, H. *Electrochem.* **2000**, *68*, 651.
(37) Gafney, H. D.; Adamson, A. W. *J. Am. Chem. Soc.* **1972**, *94*, 8238.
(38) Navon, G.; Sutin, N. *Inorg. Chem.* **1974**, *13*, 2159.
(39) Demas, J. N.; Adamson, A. W. *J. Am. Chem. Soc.* **1973**, *95*, 5159.

In a more general approach, this work demonstrates that a simple oxidation of **2** cannot produce molecular oxygen without the help of an oxygen donor. So it cannot be considered as a real functional synthetic model of the OEC of PSII.

Although **4** does not oxidize water, it is a remarkable powerful oxidant with a reduction potential of about 0.9 V vs Ag/AgCl (0.92 vs SCE). This potential is largely higher than those of the other tetranuclear Mn_4^{IV} complexes reported for which the reduction potentials have been determined in aqueous solution:[23−25,40] $[Mn_4^{IV}O_6(L)_6]^{4+}$ ($Ep_c = 0.42$ V (bpy) and 0.50 V (phen) vs SCE, pH 4.5) and $[Mn_4^{IV}O_6(bpea)_4]^{4+}$ ($Ep_c = 0.06$ V vs SCE, pH 7). Some preliminary experiments conducted in our group have already shown that **2** catalyzes electrochemically other oxidation reactions implying more simple processes such as, for example, the oxidation of alcohols, and more detailed studies are currently underway.

(40) Dubé, C. E.; Wright, D. W.; Pal, S.; Bonitatebus, P. J., Jr.; Armstrong, W. H. *J. Am. Chem. Soc.* **1998**, *120*, 3704.

Acknowledgment. The authors thank Carole Duboc from the High Magnetic Field laboratory of Grenoble, CNRS-MPI UPR 5021, France for her help with EPR experiments, the Laboratoire d'Etude Dynamiques et Structurales de la Sélectivité, UMR CNRS 5616, Université Joseph Fourier Grenoble, and the Département de Recherche Fondamentale sur la Matière Condensée, Service de Chimie Inorganique et Biologique, CEA-Grenoble for EPR access facilities.

Supporting Information Available: Cyclic voltammograms of **2** in H_2O + 0.1 M $NaBF_4$ and after exhaustive oxidation (Figure S1), cyclic voltammograms of **4** in H_2O + 0.1 M KCF_3SO_3 (Figure S2), UV−visible absorption spectra of **2** and after exhaustive reduction (Figure S3), and visible absorption spectra of **3** after the entire formation of **4** (Figure S4). This material is available free of charge via the Internet at http://pubs.acs.org.

JA052595+